Fracture Behavior of Surface-Cracked Tension Elements

CHARLES E. FEDDERSEN*
Columbus Laboratory, Battelle Memorial Institute, Columbus, Ohio

The crack length dimension is used as the principal measure of surface flaw severity to model fracture behavior in the elastic-plastic range of material behavior. Using the results of previous observations, it is shown that a single, continuous stress-crack length curve can be created for flaw shape ratios, $a/2c$, between 0.25 and 0.50, which are those most commonly encountered in structural service. The technique is verified by graphical displays of data on steel and titanium materials from several investigators.

Introduction

THE surface flaw or part-through-the-thickness crack is probably the most commonly encountered flaw in structural service. Although this flaw configuration has been studied extensively, its complex behavior is not well understood from a theoretical perspective and has hindered the development of standardization of part-through crack specimens and testing procedures. Nevertheless, because this type of flaw is a continuing "real life" problem in tankage and other structure, it retains a strong, practical precedence in materials research studies. It now appears that several recent developments can provide more engineering insight to surface flaw behavior. The development and verification of a new surface flaw fracture model is the purpose of the following presentation.

The surface flaw stress intensity factor (SIF) was first formulated by Irwin[1] in the form

$$K = S(\pi a)^{1/2}/\Phi \tag{1}$$

where S = gross stress, a = crack depth, Φ = elliptic integral. The analysis was based on the assumption of a semielliptical flaw occurring at the surface of a semi-infinite, ideally elastic medium. From this flaw model Tiffany and Masters[2] developed an extensive engineering philosophy for crack propagation and fracture.

Subsequently, these concepts and procedures have been widely adopted by many investigators. The associated bibliography is too extensive to be mentioned here. It is sufficient to note that the basic concepts appear sound and have been well substantiated. However, it is also important to recognize that there exist some alternate perspectives which have an even greater potential for unifying damage concepts in crack behavior studies.

Alternate Surface Flaw Formulation

It has been noted[3] recently that there is a rational analytical basis for formulating the surface flaw SIF in terms of the crack length. This alternate formulation is

$$K = S(\pi c)^{1/2}\theta \tag{2}$$

where S = gross stress, c = crack half-length, θ = shape factor as illustrated in Fig. 1. The similarity of expression (2) and the elementary center-crack SIF,

$$K = S(\pi c)^{1/2} \tag{3}$$

immediately suggests that concepts used in analyzing center-cracked tension panels may be generalized to describe surface flaw behavior. Such an extension is described next.

Analytical Development

A rational engineering model of surface flaw behavior is developed in this section. First, the highlights of a previously derived center-cracked tension panel analysis are reviewed. Then the key features of that analysis are generalized to model surface flaw behavior.

Center-Cracked Tension Panels

An engineering evaluation[4] of center-cracked tension panel behavior has demonstrated that linear tangents are effective cutoffs to the idealized elastic instability curve for modeling plasticity and finite width effects in fracture data. This technique was a phenomenological development based on observations of actual experimental data. The details essential to this presentation are summarized in the following paragraphs.

The analytical model which was developed and verified is illustrated in Fig. 2. The central, saddle shaped portion of the curve represents the basic elastic instability relationship,

$$S_f = K_f(\pi c)^{-1/2} \tag{4}$$

where S_f = gross fracture stress, K_f = characteristic material toughness. This is an adequate representation of center-cracked tension panel data whose net-section stress conditions are well within the elastic range ($S \leq \frac{2}{3}$ TYS and $2c \leq W/3$).

The left-hand, linear tangent, as expressed by

$$S_f = \text{TYS}(1 - 2c/W_m) \tag{5}$$

where W_m = a characteristic constant, implicitly dependent upon K_f and TYS, represents the relatively high-stress conditions associated with small flaws. This tangent models the effects of plasticity which are accentuated as the applied

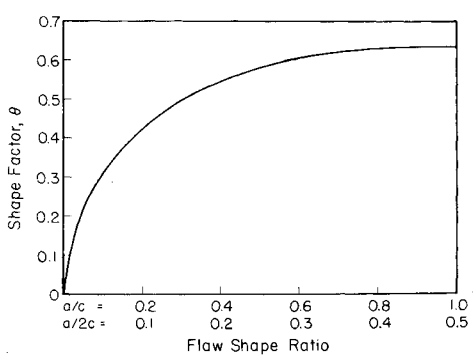

Fig. 1 The shape factor θ as a function of flaw shape ratio.

Presented as paper 71-371 at the AIAA/ASME 12th Structures, Structural Dynamics and Materials Conference, Anaheim, Calif., April 19–21, 1971; submitted March 26, 1971; revision received July 19, 1971.

Index category: Aircraft Structural Design; Structural Static Analysis; Launch Vehicle and Missile Structural Design.

* Senior Research Engineer. Member AIAA.

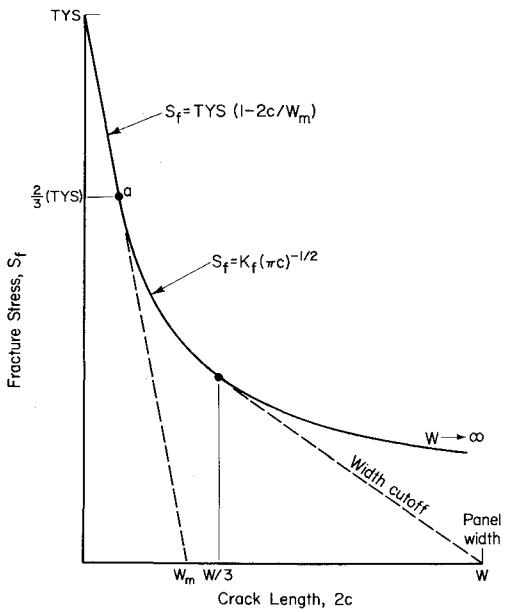

Fig. 2 Center-cracked tension panel model.

stresses approach the tensile yield strength, TYS, of the material. Expression (5) is the key equation generalized in the next section to model surface flaw behavior in the elastic-plastic region.

The right-hand linear tangent represents the relatively low-stress conditions associated with large flaws, and influenced by the panel boundary ("finiteness" of width). Generally speaking, this aspect of center-cracked tension panel analysis is of lesser importance for the surface flaw model since length dimensions of surface flaws are usually less than one-third the panel or specimen width. The validity of this technique has been substantiated by the consistency with which it fits a variety of experimental data reported by many investigators. The adaptation of this method to model surface flaw behavior is evolved in the next section.

Surface Flaw Model

An approach to surface flaw analysis is developed in analogy to that for center-cracked tension panels as summarized in the preceding section. The objective is to obtain a smooth and continuous stress-flaw size relation for the full range of real crack lengths. First, the condition of idealized elastic instability in surface flaws is considered wherein expression (2) is used directly. Then, a model of small crack behavior at high stresses is created for the left most limit where plasticity effects must be accounted for in a manner similar to that accomplished with linear tangents in the center crack analysis. In fact, the evidence that small flaw behavior transcends the elastic range must be accommodated also. Finally, these two elements are combined into a unique relationship by a tangency criterion.

Ideal elastic behavior

In a manner analogous to the center-cracked tension panel analysis, the surface flaw SIF formulation of expression (2) can be used to represent ideal elastic fracture behavior. In this expression the shape factor θ can be considered to be simply a scalar coefficient. In fact, from Fig. 1 it can be seen that the shape factor θ attains a quasistable value over the commonly encountered range of shape ratios,

$$0.25 \leq a/2c \leq 0.50, \text{ or } 0.5 \leq a/c \leq 1.0$$

hereinafter referred to as normally shaped flaws. Within this range, the shape factor θ is limited to

$$0.58 \leq \theta \leq 0.64$$

Thus, for a practical range of surface flaw shapes, an average shape factor value of

$$\theta = 0.61$$

is a representative coefficient with less than 5% error. For ideal elastic fracture under these conditions, expression (2) becomes

$$K_f = 0.61 S_f(\pi c)^{1/2} \tag{6}$$

Although this expression will be used in the subsequent analysis, other ranges of shape ratios could be studied merely by adjusting the leading coefficient.

Limiting elastic-plastic behavior

For modeling small flaw behavior at high stress levels, the left-hand linear tangent of the center-cracked model as defined by expression (5) can be generalized to reflect flaw area properties by factoring both numerator and denominator of the right-most term by the panel thickness, t. The resulting expression,

$$S_f = \text{TYS}[1 - (2c \cdot t)/(W_m \cdot t)] \tag{7}$$

may be converted to

$$S_f = \text{TYS}(1 - A_f/A) \tag{8}$$

where

$$A_f = 2c \cdot t = \text{flaw area}$$

$$A = W_m \cdot t = \text{a characteristic area}$$

Now, since the flaw area of a semielliptical surface flaw is

$$A_f = \pi ac/2 \tag{9}$$

substitution of expression (9) into expression (8) yields

$$S_f = \text{TYS}(1 - \pi ac/2A) \tag{10}$$

and a shape conversion has been achieved. The crack depth dimension may be suppressed by rewriting expression (10) as

$$S_f = \text{TYS}(1 - Hc^2) \tag{11}$$

where $H = (\pi/2A)(a/c)$. This makes the flaw shape ratio a/c a direct parameter, and eliminates crack depth as an explicit dimension. From this point on, H is considered merely as a modeling parameter to characterize surface flaw behavior. Further insight to its deeper physical or analytical nature, and to its real relationship to W_m in center-cracked tension panels is beyond the scope of this discussion.

To transcend the elastic range, it is necessary to recognize that there is a basic geometric difference in the limiting configuration of surface flaws and center cracks. This is illustrated in Fig. 3. As flaw size decreases, the surface flaw tends to vanish into a point defect. In contrast, the center crack approaches a line defect. This difference suggests that, as surface flaw size decreases, the strength of the tension element can approach the tensile ultimate strength, TUS, of the base material. However, the limiting line defect for the center crack configuration represents a more severe discontinuity

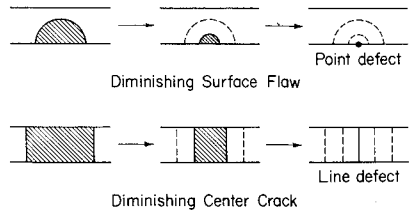

Fig. 3 Limiting flaw configurations.

where TYS is probably a more conservative limiting stress. In physical reality, the basic criterion at this limit appears to be a flow stress; however, that is beyond the scope of this discussion. By this argument, the use of TUS as a material strength limit for surface flaws is a valid substitution for the TYS limit used in center-crack analysis. Thus, expression (11) can be further converted to

$$S_f = \text{TUS}(1 - Hc^2) \tag{12}$$

With this expression, the initial linear portion of the center-cracked tension panel model has been transformed into a parabolic curve to represent small surface flaw behavior. It is also interesting to note that this is the same type of elastic-plastic cutoff used for column instability curves.

Tangency criterion

The elastic and the elastic-plastic segments of the surface flaw model are now unified by the tangency of expressions (6) and (12). The slope of the K curve of expression (6) at any point is

$$\begin{aligned} dS_f/d(2c) &= d[1.64K_f(\pi c)^{-1/2}]/d(2c) \\ &= -S_f/4c \end{aligned} \tag{13}$$

The slope of any point on the elastic-plastic segment of expression (12) is

$$\begin{aligned} dS_f/d(2c) &= d[\text{TUS}(1 - Hc^2)]/d(2c) \\ &= (\text{TUS})Hc \end{aligned} \tag{14}$$

Equating these two slopes to define a tangency point a yields

$$S_f|_a = (\text{TUS})4Hc^2 \tag{15}$$

which defines the stress level at which tangency occurs. Substitution of expression (15) into expression (12) reveals that

$$S_f|_a = 0.8\text{TUS} \tag{16}$$

is the stress level associated with the tangency point a. This implies that the elastic instability relation of expression (6) is valid to 80% of TUS above which the elastic-plastic curve of expression (12) is a better representation of fracture behavior.

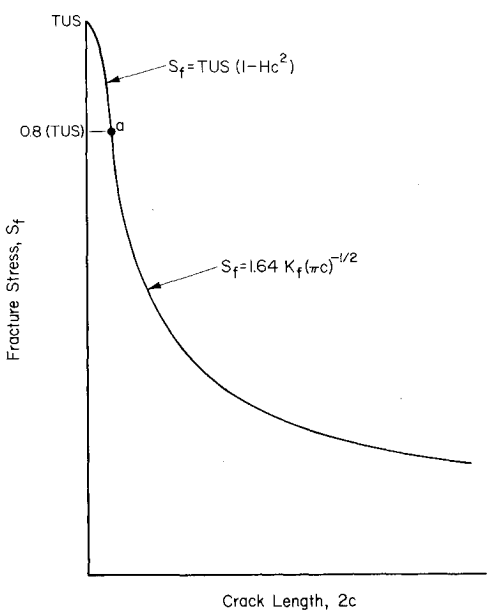

Fig. 4 Illustration of the surface flaw model.

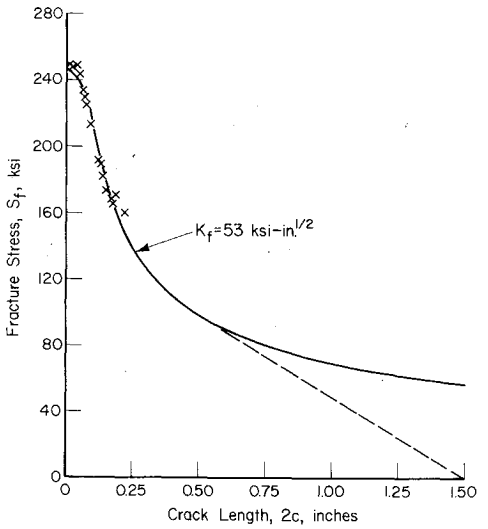

Fig. 5 Surface flaw fracture in 0.110 in. thick, 1.5 in. wide 4340 steel sheet at room temperature.[5]

Rules of the method

This development may be summarized in the following "set of rules" which define the basic segments of the complete stress-flaw size curve. In the elastic range below 80% of TUS,

$$S_f = 1.64K_f(\pi c)^{-1/2} \tag{17}$$

is the appropriate data model for normally shaped flaws. For transcending the elastic range limit of 80% of TUS, the flaw behavior model is

$$S_f = \text{TUS}(1 - Hc^2) \tag{18}$$

where $H = 0.112(\text{TUS}/K_f)^4$ is the parameter which results from equating expressions (17) and (18) at the tangency point a. This is graphically illustrated in Fig. 4.

Verification of the Surface Flaw Model

The analytical developments of the previous section have been applied to a variety of experimental data reported by several investigators. The resulting correlations are illustrated in Figs. 5–11 and are discussed in the following paragraphs. The data presented are for the shape ratio range,

$$0.25 \leq a/2c \leq 0.50$$

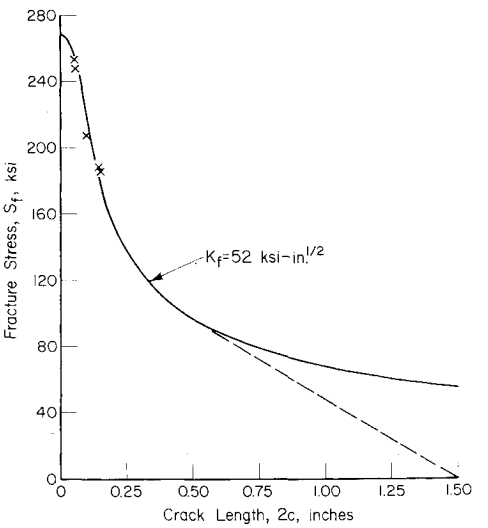

Fig. 6 Surface flaw fracture in 0.135 in. thick, 1.5 in. wide 4340 steel plate at room temperature.[6]

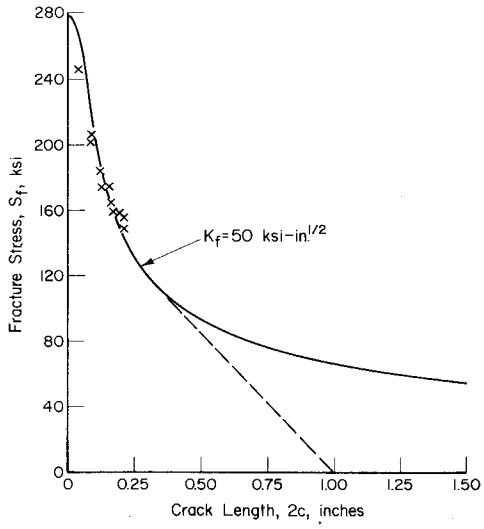

Fig. 7 Surface flaw fracture at $\frac{1}{4}$ in. thick, 1 in. wide 4340 steel plate at room temperature.[7]

and, in general, for crack depth/thickness ratios,

$$a/t \leq 0.50$$

such that the effect of the second or back surface is negligible. Because of these geometries a width effect is not usually evident. However, for clarity of presentation the appropriate width cutoffs for the particular specimen size are included on the figures as a dashed line tangent to the K_f curve.

In the following data analysis only the elastic data, i.e., data whose fracture stress was less than or equal to 80% TUS, have been used to derive the analytical curve. Expression (6) was used with these data to compute a simple average K_f value. Then, the stress relations of expressions (17) and (18) were used to create the continuous curves. The power of this model can be noted visually by the close fit of data above 80% of TUS to a line based on and projected from data lying below 80% of TUS. In practical applications, it would also be appropriate to weigh in the elastic-plastic data.

Fracture data of relatively thin 4340 steel sheet with 245 ksi TUS are presented in Fig. 5. Of particular interest is the excellent fit of data to the analytically derived curve through the elastic-plastic range. The K_f value of 53 ksi-in$^{1/2}$ is the simple average value of toughness computed for the data below 80% of TUS. Some supporting, Battelle derived data

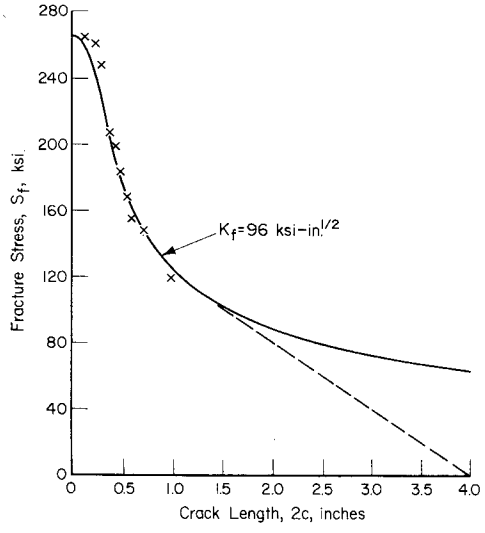

Fig. 8 Surface flaw fracture in $\frac{3}{4}$ in. thick, 4 in. wide 18% nickel maraging steel at room temperature.[8]

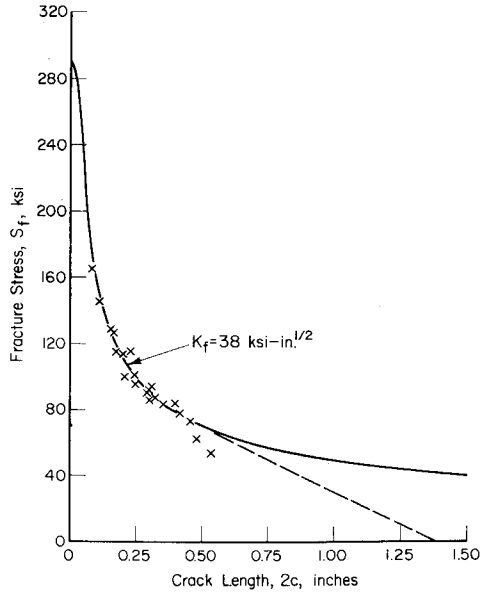

Fig. 9 Surface flaw fracture in $\frac{1}{4}$ in. thick, 1.4 in. wide D6AC steel plate at room temperature.[9]

are shown in Fig. 6. These represent a slight increase in sheet thickness and a higher TUS level of 268 ksi. A comparable toughness value of 52 ksi-in$^{1/2}$ is obtained. In Fig. 7, fracture data for a greater thickness of 4340 steel is shown. The TUS is 278 ksi. The K_f value is slightly depressed from the two previous illustrations, possibly affected by both thickness and strength. A good data fit is indicated. Another very good fit of fracture data is shown in Fig. 8. This is an 18% nickel maraging steel with a TUS of 266 ksi. It appears distinctly tougher than the previously illustrated 4340 materials, even though the thickness is greatly increased. Figure 9 presents fracture data for D6AC steel at 289 ksi TUS. These data include a diverse variety of flaw forms, all of which correlate well on this data format. Of particular interest is the good fit to the central, saddle-shaped, ideal K curve.

In Fig. 10, some Ti-6A1-4V STA titanium alloy fracture data are presented to demonstrate that these analytical techniques are also applicable for other metallic materials. Note the good fit of data over the entire stress range. Finally, some cryogenic data for another titanium alloy are shown in Fig. 11. These are fracture data from two different width specimens of Ti-5A1-2.5Sn titanium alloy sheet. These

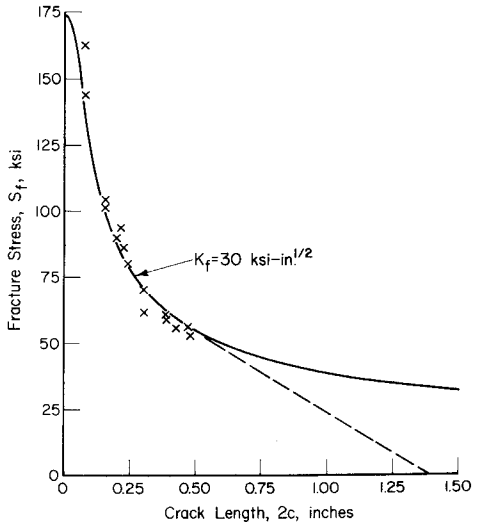

Fig. 10 Surface flaw fracture in $\frac{1}{4}$ in. thick, 1.4 in. wide Ti-6A1-4V STA titanium alloy plate at room temperature.[9]

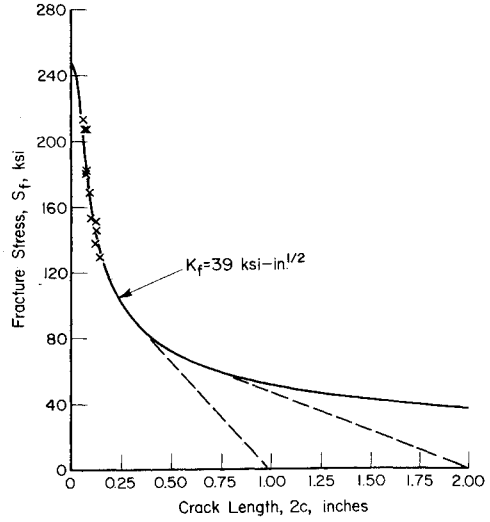

Fig. 11 Surface flaw fracture in 0.060 in. thick, 1 and 2 in. wide Ti-5Al-2.5Sn ELI titanium alloy plate at −423°F.[10]

figures substantiate the validity of the analytical model which has been developed.

Conclusions and Future Work

An engineering model of surface flaw fracture behavior based on a new formulation of the surface flaw SIF has been developed and verified. A smooth and continuous curve of stress and flaw size can be generated in the elastic stress range and projected through the plastic stress range to the TUS of the material (at zero flaw size). Implicit to its correlation of elastic instability data, this evaluation has also validated the adequacy of the new formulation of the surface flaw SIF. Most importantly, however, it provides a means of representing flaw behavior in the elastic-plastic stress transition.

An important aspect of this analysis is its foundation in the phenomenological development of an earlier center-cracked tension-panel analysis. Each model complements the other and implies an even more basic interdependency. The nature of this fundamental relationship is the subject of continuing Battelle research in this area.

References

[1] Irwin, G. R., "Crack-Extension Force for a Part-Through Crack in a Plate," *Journal of Applied Mechanics*, Vol. 84, No. 4, Dec. 1962, pp. 651–654.

[2] Tiffany, C. F. and Masters, J. N., "Applied Fracture Mechanics," *Fracture Toughness Testing and its Applications*, Special Technical Publication 381, American Society for Testing and Materials, Philadelphia, 1965, pp. 249–277.

[3] Feddersen, C. E., "A Note on the Formulation of the Surface Flaw Stress Intensity Factor," *International Journal of Fracture Mechanics*, Vol. 7, No. 1, March 1971, pp. 111–115.

[4] Feddersen, C. E., "Evaluation and Prediction of the Residual Strength of Center Cracked Tension Panels," *Damage Tolerance in Aircraft Structures*, Special Technical Publication 486, American Society for Testing and Materials, Philadelphia, 1971, pp. 50–78.

[5] Kerlins, V. and Pendleberry, S. L., "The Effect of Crack Type and Material Thickness on the Fracture Strength of 4340 Steel," SM-43113, Oct. 1963, Douglas Aircraft Co., Santa Monica, Calif.

[6] Hoeppner, D. W., Feddersen, C. E., and Pettit, D. E., "Summary Report to Babcock and Wilcox Research Center," Nov. 1, 1967, Battelle Memorial Inst., Columbus, Ohio.

[7] Corn, D. L., "Effect of Crack Shape on PTC Fracture Toughness Behavior," SM-49149, Jan. 1966, Douglas Aircraft Co., Santa Monica, Calif.

[8] Corn, D. L., "Evaluation of 18Ni-9Co-5Mo (300 ksi) Maraging Steel Sheet, Part 1: Mechanical Properties," SM 43110, Nov. 1963, Douglas Aircraft Co., Santa Monica, Calif.

[9] Randall, P. N., "Severity of Natural Flaws as Fracture Origins, and a Study of the Surface Cracked Specimen," AFML-TR-66-204, Aug. 1966, TRW Systems, Redondo Beach, Calif.; also *Plane Strain Fracture Toughness Testing of High Strength Metallic Materials*, Special Technical Publication 410, American Society for Testing and Materials, Philadelphia, 1966, pp. 88–125.

[10] Orange, T. W., Sullivan, T. L., and Calfo, F. D., "Fracture of Thin Sections Containing Through and Part-Through Cracks," TM X-52794, June 1970, NASA.